FR 82 0 3116

institut de physique nucléaire

LABORATOIRE ASSOCIÉ A L'IN2P3

IPNO-DRE-82-17

DIRECT TRANSFER AND TWO-STEP PROCESSES IN THE $^{42}Ca(\alpha,{}^{3}He)^{43}Ca$ REACTION.

E. Hourani, S. Fortier, J.M. Maison,
S. Galès and J.P. Schapira.

UNIVERSITÉ PARIS-SUD

IPNO-DRE-82-17

DIRECT TRANSFER AND TWO-STEP PROCESSES IN THE $^{42}Ca(\alpha,{}^{3}He)^{43}Ca$ REACTION.

E. Hourani, S. Fortier, J.M. Maison,
S. Galès and J.P. Schapira.

DIRECT TRANSFER AND TWO-STEP PROCESSES IN THE $^{42}Ca(\alpha,{}^{3}He)^{43}Ca$ REACTION

E. Hourani, S. Fortier, J.M. Maison, S. Galès and J.P. Schapira

Institut de Physique Nucléaire BP N°1, 91406 Orsay, France.

Abstract :

The $^{42}Ca(\alpha,{}^{3}He)^{43}Ca$ reaction has been studied at 36 MeV incident energy. Angular distributions have been measured from 4° to 42° using a split-pole spectrometer and position sensitive Si detectors, for about 40 levels located up to 6 MeV excitation energy. A local zero-range DWBA analysis has been carried out; ℓ = 3 and 4 - assignments are tentatively proposed for levels located above 4 MeV excitation energy, indicating a strong fragmentation of the $1f_{5/2}$ strength between 4 and 6 MeV and the location of the main component of the $1g_{9/2}$ strength above 6 MeV. A number of weakly excited levels cannot be reproduced by DWBA analysis. Their angular distributions have been compared with the results of coupled-reaction-channel calculations assuming two-step excitation of weak coupling states with a $[^{42}Ca^{*} \otimes f_{7/2}]$ structure. A reasonable agreement has been obtained, confirming that the two-step process cannot be neglected in the analysis of $(\alpha,{}^{3}He)$ reaction.

[NUCLEAR REACTIONS $^{42}Ca(\alpha,{}^{3}He)^{43}Ca$, E = 36 MeV; measured $\sigma(E,\theta)$. ^{43}Ca deduced levels ℓ,S.DWBA and CRC analysis. Enriched target.]

1. Introduction

Information about the location and the fragmentation of neutron single-particle strengths has been mainly obtained by means of the (d,p) reaction at low incident energy, and it is, generally, mostly limited to low spin orbitals. Such a fact is easily understood by considering the strong angular mismatch encountered in this reaction for $\ell > 2$ transfers, inducing small cross sections for excitation of levels with a higher ℓ-value and thus making somewhat dubious the results of a standard DWBA analysis. Consequently, the (α,^{3}He) reaction appears to be complementing the (d,p) one as a spectroscopic tool, as from semi-classical arguments it is expected to favor higher ℓ-transfers. In particular, it could be hoped that the study of this reaction on calcium isotopes would give useful information about the distribution of the $1f_{5/2}$ and $1g_{9/2}$ neutron single-particle strengths whereas most of the available data from (d,p) results concern the $2p_{3/2}$ and $2p_{1/2}$ orbitals.

In our recent study[1] of the ^{40}Ca(α,^{3}He)^{41}Ca reaction at 36 MeV incident energy, it has been shown that, apart from the very strong direct transition to the $7/2^-$ ground state and a few $\ell = 3$ and 4 direct transfers to previously known $5/2^-$ and $9/2^+$ levels, we have observed several transitions to well-identified core-excited states with a $[^{40}Ca^* \otimes f_{7/2}]$ structure. In most cases, the corresponding experimental angular distributions characterized by a spin-dependent pattern could not be reproduced by assuming a direct one-step process, whereas coupled reaction-channel (CRC) calculations involving pure two-step mechanisms gave a much better agreement with the data. Such an experiment has emphasized the contribution of two-step processes in (α,^{3}He) reaction showing that they should be included in the analysis in order to get more confident results.

In the present paper, we report on a $^{42}Ca(\alpha,{}^{3}He)^{43}Ca$ reaction performed under the same experimental conditions as in our previous $^{40}Ca(\alpha,{}^{3}He)^{41}Ca$ study, here denoted as Paper I, and a priori complementing two previous $^{42}Ca(d,p)^{43}Ca$ studies[2,3]. The results of the DWBA analysis will be presented in section 3 and compared to the data, with a tentative identification of $1f_{5/2}$ and $1g_{9/2}$ strength fragments in ^{43}Ca below 6 MeV excitation energy. In section 4, experimental angular distributions for both previously known[4,5] low spin ($1/2^+$ and $3/2^+$) and high spin ($11/2^+$, $13/2^+$, $9/2^-$, $11/2^-$ and $13/2^-$) states will be compared with CRC calculations involving two-step excitation (inelastic scattering + neutron transfer) of core-excited states with a $[^{42}Ca^{*} \otimes f_{7/2}]$ structure.

2. Experimental procedure

The $^{42}Ca(\alpha,{}^{3}He)^{43}Ca$ reaction has been studied at 36 MeV incident energy with the Orsay MP tandem. The 95 % isotopically enriched ^{42}Ca target backed by a 10 $\mu g/cm^2$ carbon film was about 160 $\mu g/cm^2$ thick. The ^{3}He particles were detected as in Paper I by six position sensitive Si detectors located in the focal plane of a split-pole magnetic spectrograph and discriminated from other light particles of the same ρB value by their energy losses in the Si detectors. The overall energy resolution was 20 keV. Energy spectra of the ^{3}He were recorded in 4° steps from 4° to 42°. Two successive exposures at different magnetic fields were necessary at each angle to cover the spacings between adjacent detectors. The absolute cross sections were obtained by measuring the elastic cross sections of the α-particles on the ^{42}Ca target at 10° and 12° and comparing them with optical model predictions. The resulting uncertainty on the cross sections is estimated to be about 15 %. An accurate calibration in excitation energy was carried out in a subsequent run using a 50 cm delay line gaz counter. The peak positions along the counter for the six lowest levels in ^{43}Ca of well-known excitation energy were observed at various values of the magnetic field. The obtained accuracy in the determination of excitation energies is estimated to be about 8 keV. A spectrum recorded at 14° lab angle with the gaz counter is shown in Figure 1. The numbers at the top of the peaks in Fig. 1 refer to nuclear levels in ^{43}Ca whose corresponding excitation energies are listed in Table 1. About forty levels were resolved up to 6 MeV excitation energy. The accurate determination of their energy allowed to identify most of them with levels of known spin values given in Refs. 4 and 5, a fact which made our two-step analysis feasible. A number of levels located between 4 and 6 MeV in excitation energy are observed for the first time and may correspond to $1f_{5/2}$ and $1g_{9/2}$ single-particle fragmentated strengths, as discussed in the next section.

3. Distorded-wave analysis

3.1 DWBA calculations

The calculations of the theoretical angular distributions were made in the DWBA theory of direct reactions using the code DWUCK[6] with the zero-range, local approximation. Single-particle wave functions taken as form factors were generated in the usual procedure by adjusting the depth of the Woods-Saxon well in order to reproduce the experimental separation energies. The geometrical parameters of the well are listed in Table 2. The optical protential for ^{3}He taken from Bechetti and Greenless[7] is also given in Table 2. As for the α optical potential, there exists a large number of α-elastic scattering analyses on Ca isotopes with resulting optical parameters (compiled by Perey[7]) corresponding to a standard Woods-Saxon shape. However, it has been recently shown[8,9] that α-elastic scattering data at backward angles (ALAS effect) could be reproduced in a coherent way for a wide range of isotopes and energies, only by assuming a different shape for the real part in the α-potential described by a (Woods-Saxon)$^{\nu}$ form factor where ν can vary between 2 and 5.

It was of interest to try in transfer reaction,in addition to the traditional α-potentials of Woods-Saxon shape (denoted here by W.S), that of (W-S)$^{\nu}$ shape (denoted here by (W-S)$^{\nu}$). Different sets of both types of potentials given in the Refs [7-9] for masses and energies close to 42 and 36 MeV respectively were used; the corresponding calculated angular distributions were compared with experimental angular distributions of different known ℓ-transfers taken from this work and from Paper I. Typical results were obtained, which are illustrated in Fig. 2, where are presented two sets of data on ^{40}Ca and ^{42}Ca targets and the theoretical corresponding distributions calculated with two α-potentials (reported in Table 2) that we adopted. The first adopted potential of W-S form in the same as the potential used in Paper I; it well reproduces the experimental data for ℓ = 1 and 3 up to 4 MeV excitation energy, but it gives poor fits to ℓ = 3 angular distributions above 4 MeV in ^{43}Ca and to ℓ = 4 distributions in ^{43}Ca and ^{41}Ca. The second adopted potential has a (W-S)^{2} form factor in its real part; it better reproduces the forward angles in ℓ = 3 transfer above 4 MeV excitation energy in ^{43}Ca and in particular it fits the ℓ = 4 experimental distributions with their characteristic enhancement at 30°, but it gives a poor fit for the ℓ = 3 transfer to g.s. and out of phase angular distributions in ℓ = 1 transfer case. Consequently, the W-S potential was chosen to extract the spectroscopic factors listed in Table 1 and to perform CRC calculations, whereas the (W-S)^{2} one was used, only qualitatively, to give some confidence in a tentative ℓ-assignment to levels located at high excitation energy ($E_x \gtrsim 4$ MeV).

3.2 Comparison with the data

Angular distributions computed for $\ell = 1$ to 4 angular momentum transfer are compared with experimental data in Figures 3 and 4. The spectroscopic factors (2J+1)S were extracted from experimental cross sections $d\sigma/d\Omega$ by means of the expression :

$$\left.\frac{d\sigma}{d\Omega}\right)_{exp} = N\ (2J+1)\ S\ \sigma_{DW}^{\ell j}$$

where $\sigma_{DW}^{\ell j}$ is the cross section calculated by DWUCK and N is the normalization factor for (α,^{3}He) reaction which was taken equal to the commonly used value 46. The accurate determination of the target thickness in this experiment and the originally known isotopic percentage of ^{40}Ca isotope in our target permitted the determination of the absolute cross sections in the reaction ^{40}Ca(α,^{3}He) leading to the ground state of ^{41}Ca. Comparing this result with the one of Paper I improved the determination of the thickness of the ^{40}Ca target in Paper I and gave for N a value of about 46 instead of 34 (see Ref. 1) corresponding to the transition ^{40}Ca(α,^{3}He)^{41}Ca$_{g.s.}$ with a spectroscopic factor S = 1.

The results of the DWBA analysis are reported in Table 1, together with those obtained in previous (d,p) reactions[2,3]. The extracted value of 5.40 for the ground state is in a good agreement with previous results and exhausts 90 % of the $1f_{7/2}$ shell model sum rule. It is worth noting that the realistic values of S found for ^{43}Ca g.s. as well as for ^{41}Ca g.s. give confidence in the value 46 used herein for N, which was not, nevertheless, adopted in recent works[10,11] on Sm(α,^{3}He) reaction at 40 MeV.

There are two $2p_{3/2}$ states at 0.593 and 2.046 MeV and one $2p_{1/2}$ state at 2.611 MeV which are clearly evidenced and correspond to the strongest $\ell = 1$ levels among the large number of observed $\ell = 1$ transitions in (d,p) reactions. The observation of a few $\ell = 2$ weak transitions illustrates the incomplete closure of $1d_{3/2}$ and $1d_{5/2}$ orbitals in ^{42}Ca.

The good matching for $\ell = 3$ at low excitation energy has evidenced a single-particle contribution to the $5/2^-$ state at 0.373 MeV and gives confidence in the small values of (2J+1)S obtained for the known ($5/2^-$, $7/2^-$) states at 2.674, 3.413 and 3.804 MeV; the $1f_{5/2}$ strength is therefore believed to be mainly located above 4 MeV. In Figure 4, are displayed five levels of similar shape, one of them, at 4.463 MeV, being previously determined as $\ell = 3$. We have not displayed in the same figure the angular distributions corresponding to the levels at 4.041, 4.880, 5.040, 5.410, 5.548, 5.727, 5.805 and 5.889 MeV, which all have a similar shape but poorer angular distributions due either to small cross sections on a growing background or to the presence of contaminants peaks. Some of them consist of doublets or multiplets of states. All these states, displayed or not, are tentatively assigned as $\ell = 3$ and presumably reflect a strong fragmentation of the $1f_{5/2}$ strength between 4 and 6 MeV in excitation energy. The $(W-S)^2$ α-potential calculations reproduce the forward angles slightly better than the (W-S) ones; however, each of the selected potentials give for these states a sum of spectroscopic strengths exceeding 10, i.e. 160 % of the shell model sum rule. This too high value may be due to the mismatch of $\ell = 3$ transfer above 4 MeV which renders the extraction of spectroscopic strengths less confident.

The $(W-S)^2$ α-potential calculations performed with $\ell = 4$ transfer reproduce the angular distributions of the level at 3.193 MeV known as

$(3/2-13/2)^+$; it is therefore tentatively assigned as a $1g_{9/2}$ transition. The states at 3.278 and 3.913 MeV are unresolved doublets and seem to contain an important contribution of $\ell = 4$. The identification of the state at 4.123 MeV as $\ell = 4$ is in agreement with (d,p) results. All these states tentatively identified as $\ell = 4$ give small spectroscopic factors and would simply indicate the beginning of a fragmentated $1g_{9/2}$ strength located above 6 MeV excitation energy.

4. Coupled-reaction-channel analysis (CRC)

4.1 Calculations

Several weakly excited states, most of them with high spin known values, have been evidenced in this work and their angular distributions could not be reproduced by a direct transfer calculation. A CRC calculation, similar to the one performed Paper I, was carried out, involving a two-step process by coupling the inelastic excitation of both target and residual nuclei with neutron pick-up.

The ^{43}Ca states under study in this section being mostly located below 4 MeV excitation energy, only the first strong collective 2^+, 3^-, 4^+ and 5^- states excited in inelastic ^{42}Ca (α,α') reaction are considered and coupled with $1f_{7/2}$ transfer. Further simplification is accomplished by neglecting contributions from 4^+ or 5^- states when they compete with that from 2^+ or 3^- states respectively, this simplification being supported by two arguments : 1) for an equivalent inelastic excitation of 2^+, 3^-, 4^+ and 5^- states, comparison between calculated cross sections shows that the contributions from $[2^+ \otimes f_{7/2}]$ or $[3^- \otimes f_{7/2}]$ couplingsare one order of magnitude higher than those from $[4^+ \otimes f_{7/2}]$ or $[5^- \otimes f_{7/2}]$ respectively, when performed to populate the same state in ^{43}Ca, and 2) one can notice in the ^{43}Ca (α,α') results[12] that the admixture of $\ell = 4$ or or $\ell = 5$ in the $\ell = 2+4$ or $\ell = 3+5$ transitions reaching the states under study does not exceed 20 % of the cross section.

The theoretical angular distributions are computed using the code CHUCK[13] according to two interfering one-way paths (α,α', ^{3}He) and (α, ^{3}He, ^{3}He') taken with a phase factor $(-1)^{L+j+\frac{1}{2}}$. Here, we have denoted by L the spin of the collective excited state and by j the spin of the reached level in ^{43}Ca coupled in the scheme $[L \otimes f_{7/2}]^j$. The deformation parameters describing the collective states in ^{42}Ca and their corresponding weak-coupling multiplets in ^{43}Ca are taken from Ref. 14 and reported in Table 3. The normalization factor and the spectroscopic amplitude used in the $1f_{7/2}$ - transfer are 46 and $\sqrt{0.75}$ respectively.

4.2 Comparison with the data

Two categories of spin for the weakly excited states in this work were identified by comparing with previous spectroscopic results in ^{43}Ca[4,5]. The first category consists of low values ($1/2^+$ and $3/2^+$). A direct transfer to these states is inhibited by the mismatch of the $\ell = 0$ and 2 transfer in (α,^{3}He) reaction and is, therefore, expected to be only competing with the two-step process. The second category consists of spins as high as 11/2 and 13/2 which are expected to be strongly inhibited in a direct transfer due to the high energy of the involved shell-model orbitals. The experimental distributions together with the calculated ones are displayed in Fig. 5.

4.2.1 Low spin states

The angular distributions for $1/2^+$ and $3/2^+$ states are calculated assuming a two-step process, according to the $[3^- \otimes f_{7/2}]$ coupling scheme. The $1/2^+$ state at 2.741 MeV is better reproduced than the 1.957 MeV state both in shape and in the ratio of experimental to theoretical cross sections found close to 1, a value which exhaust the weak-coupling intensity. The same coupling applied to $3/2^+$ states shows a little better fit for 2.850 MeV state, especially at large angles ($\theta > 30°$), than for 0.990 MeV state for which the direct component seems to be predominant.

4.2.2 High spin states

a) Positive parity states

The peak at 2.948 MeV has an experimental width larger than the energy resolution and consists in fact of a doublet of known states (the $3/2^-$ at 2.943 MeV and the $11/2^+$ at 2.951 MeV). The figure simply shows that the data could be fitted equally well by an $\ell = 1$ direct transfer by a two-step process with a $[3^- \otimes f_{7/2}]$ coupling.

Two $13/2^+$ states at 3.371 and 3.504 MeV could be fitted by a two-step process considering two different couplings, $[3^- \otimes f_{7/2}]$ and $[5^- \otimes f_{7/2}]$, giving a ratio of experimental to theoretical cross sections of about 0.11 and 1.76 respectively. The $[3^- \otimes f_{7/2}]$ coupling is obviously predominant.

The state at 5.251 MeV is identified with the known $(7/2 - 13/2)^+$ state located at this energy. The angular distributions calculated in two-step process assuming a $[3^- \otimes f_{7/2}]$ coupling to $7/2^+$, $11/2^+$ and $13/2^+$ spin values are displayed in the figure. Only the $7/2^+$ value is in agreement with the shape of the experimental results. The $9/2^+$ value was not considered in the two-step calculations because a direct $\ell = 4$ transfer could then compete and probably would be predominant Although a large ratio of 3.17 is obtained, a spin of $7/2^+$ is proposed for this state.

b) Negative parity states

Two known $11/2^-$ states at 1.678 and 3.044 MeV are shown in Figure 5. Their quite different shapes can be understood as follows : while the state at 3.044 MeV is explained in shape by the CRC analysis, the state at 1.678 MeV resembles closely in shape to the level observed at 4.01 MeV in Paper I and therefore could be similarly explained by a destructive interference between a two-step process with a $[2^+ \otimes f_{7/2}]$ coupling and a weak h11/2 direct transfer. The $9/2^-$ state at 3.044 MeV is well reproduced by the CRC analysis. The state at 3.645 MeV assigned as $13/2^-$ in recent studies but excited in a previous (α,α') work[12] with an $\ell = 2+4$ transition, is consistent in shape with a $13/2^-$ state as being reproduced in CRC calculations with a $[4^+ \otimes f_{7/2}]$ coupling.

5. Conclusion

The present study has investigated the $\ell = 3$ and 4 favoured direct transfers, thus complementing the previous (d,p) studies on ^{42}Ca performed at low energy in which these transfers are strongly mismatched. The experimental data give evidence for a strong fragmentation of the $1f_{5/2}$ shell-model strength between 4 and 6 MeV excitation energy and indicate that the main component of the $1g_{9/2}$ strength is located above 6 MeV.

The CRC analysis carried out to explain the weakly excited states has reproduced the shape of most of the high spin states and indicated their presence in populating the low spin states for which an $\ell = 0$ and 2 direct transfer is inhibited in $(\alpha,{}^3He)$ reaction. The rather good agreement obtained for a number of levels is consistent with the assumption that they are core-excited states implying a predominant coupling of one $f_{7/2}$ neutron with low-lying collective states in ^{42}Ca. As the shape of the theoretical two-step calculation is characteristic of the spin and parity of the final state, a value of $7/2^+$ is proposed for the level at 5.251 MeV. In agreement with the results of Paper I, it may be asserted that the CRC calculation, should not be neglected in the analysis of the (α, ^{3}He) reaction to excited states with small cross sections. However, such a CRC calculation would require a refinement by taking into account simultaneous contributions from different collective core-states and interferences with the direct transfers.

We would to acknowledge the technical staff of the Orsay Tandem for their assistance during the experiment.

References

1) S. Fortier, J.M. Maison, Ph. Picot, S. Galès, E. Hourani and J.P. Schapira, Nucl. Phys. A370 (1981) 189.

2) W.E. Dorenbusch, T.A. Belote and Ole Hansen, Phys. Rev. 146 n°3 (1966) 734.

3) G. Brown, A. Denning and J.G.B. Haigh, Nucl. Phys. A225 (1974) 267.

4) P.M. Endt and C. Van der Leun, Nucl. Phys. A310 (1978) 1.

5) A.H. Behbehani et al. J. Phys. G : Nucl. Phys. 5 n°8 (1979) 1117.

6) P.D. Kunz, University of Colorado, Report COO-535-606 (unpublished)

7) C.M. Perey and F.G. Perey, Nucl. Data Tables 19 (1977) 327.

8) Th. Delbar et al. Phys. Rev. C18 (1978) 1237.

9) H.P. Gubler, U. Kiebele, H.O. Meyer, G.R. Plattner and I. Sick, Nucl. Phys. A351 (1981) 29.

10) J. Rekstad et al., Nucl. Phys. A369 (1981) 453.

11) G. Lovhoiden et al. Nucl. Phys. A369 (1981) 461.

12) M.J.A. de Voigt, D. Cline and R.N. Horoshko, Phys. Rev. C10 (1974) 1798.

13) P.D. Kunz, private communication.

14) E.P. Lippincott and Aron M. Bernstein, Phys. Rev. 163 (1967) 1170.

Table 1 : Levels extracted in the reaction $^{42}Ca(\alpha,{}^{3}He)^{43}Ca$ at 36 MeV and the results of the DWBA analysis with α-potential of W_S type.

Present work						Previous works		
Peak no	E_x a) (MeV)	J^{π} b)	$(\frac{d\sigma}{d\Omega})_{C.M.}$ at 9° Lab. (mb/sr)	ℓ	(2J+1)S c)	ℓ	(d,p) d) 7 MeV (2J+1)S	(d,p) e) 10 MeV (2J+1)S
1	0.	$\frac{7}{2}^-$	7.0	3	5.40	3	5.4	4.4
2	0.373	$\frac{5}{2}^-$	0.105	3	0.15			
3	0.593	$\frac{3}{2}^-$	0.011	1	0.17	1	0.21	0.16
4	0.990	$\frac{3}{2}^+$	0.180	2	0.87	2	0.51	0.27
5	1.395	$\frac{5}{2}^+$	0.013	2	0.06	(2)	(0.12)	(0.03)
6	1.678	$\frac{11}{2}^-$	0.014	(CRC)				
7	1.957	$\frac{1}{2}^+$	0.023	(0) + (CRC)		0	0.13	0.10
8	2.046	$\frac{3}{2}^-$	0.093	1	- 4.26	1	2.9	2.8
9	2.249	$\frac{9}{2}^-$	0.023	CRC				
10	2.611	$\frac{1}{2}^-$	0.007	1	0.33	1	0.28	0.27
11	2.674	$(\frac{5}{2},\frac{7}{2})^-$	0.068	3	(0.28,0.18)	3	(0.14)	0.08
12	2.741	$\frac{1}{2}^+$	0.008	CRC		0	0.01	0.002
13	2.850	$(\frac{3}{2},\frac{5}{2})^+$	0.019	2 + (CRC)	(0.32,0.27)	0		0.001
14	2.948*	$\frac{3}{2}^-$ / $\frac{11}{2}^+$	0.016	(1) (CRC)	(0.74)	1	0.24	0.19
15	3.044	$\frac{11}{2}^-$	0.023	CRC				
16	3.085	$(\frac{3}{2},\frac{5}{2})^+$	0.031	2	(0.70,0.55)	(2)		
17	3.193	$(\frac{3}{2}-\frac{13}{2})^+$	0.067	4	(0.10)			

Table 1 (continued)

18	3.278*	$(\frac{7}{2}\frac{13}{2})^+$	0.080	(4)	(0.13)	1	0.21	0.12
19	3.371	$\frac{13}{2}^+$	0.018	CRC				
20	3.413	$(\frac{5}{2},\frac{7}{2})^-$	0.065	3	(0.43,0.29)	3		0.19
21	3.504	$\frac{13}{2}^+$	0.025	CRC				
22	3.645	$\frac{13}{2}^-$	0.019	CRC				
23	3.803		0.030	(3)	(0.20)	(3)	(0.16)	
24	3.913*		0.062	(4)	(0.14)	4	1.12	
25	4.041	$(\frac{3}{2},\frac{5}{2})^+$	0.029			2		0.01
26	4.123	$(\frac{7}{2},\frac{9}{2})^+$	0.017	(4)	(0.04)	4		0.19
27	4.193	$\frac{1}{2}^-$	0.004	1	0.44	1	0.86	0.84
28	4.463		0.094	(3)	(1.45)	3	0.35	
29	4.569							
30	4.826		0.037	(3)	(0.90)			
31	4.880		0.022					
32	5.001		0.052	(3)	(1.16)			
33	5.040		0.018					
34	5.200		0.120	(3)	(2.80)			
35	5.251	$(\frac{7}{2}\frac{13}{2})^+$	0.018	CRC				
36	5.410		0.006					
37	5.548*		0.035					
38	5.647*		0.012					
39	5.727*		0.025					
40	5.805		0.022					
41	5.889*		0.027					
42	5.991		0.049	(3)	(2.75)			

a) The accuracy on excitation energies is about 8 keV. The values of E_x marked by an asterisk correspond to doublets of levels.

b) Refs.[4,5]

c) When two values are given, they correspond to the two given values of J^π respectively. The values given for $\ell = 4$ are calculated in the hypothesis of $1g_{9/2}$ and those for $\ell = (3)$ in the hypothesis of $1f_{5/2}$.

d) Ref.[2]; e) Ref.[3].

Table 2 : Optical potentials used in the analysis of the $^{42}Ca(\alpha,{}^{3}He)$ reaction at 36 MeV.

Particle	Potential type	V_o (MeV)	r_o (fm)	a_o (fm)	W (MeV)	r'_o (fm)	a'_o (fm)	r_c (fm)
n[a]		U_o	1.25	0.65				
^3He[b]		V_{BG}	1.20	0.72	W_{BG}	1.40	0.88	1.3
α[c]	W-S	180	1.35	0.65	23.5	1.31	0.69	1.3
	$(W-S)^2$	202.2 −0.304E	1.35	1.32	49.6 −0.511E	0.147 +0.02E	1.10	1.3

a) The n form factors are calculated with a binding potential

$$U(r) = -U_o[f(r,r_oA^{1/3},a_o) - \frac{\lambda}{45.2}\frac{1}{r}\frac{d}{dr} f(r,r_oA^{1/3}, a_o)\ \vec{L}.\vec{S}]$$

with $f(r,r_oA^{1/3}, a_o) = 1/[1+\exp(r-r_oA^{1/3})/a_o]$

and $\lambda = 25$.

b) $V_{BG} = 151.9 - 0.17E + 50(N-Z)/A$; $W_{BG} = 41.7 - 0.33E + 44(N-Z)/A$ taken from Ref.[7].

c) The W-S type is of the form : $V(r) = V_c - V_of(r,r_o\ A^{1/3},a_o) - iWf(r,r_oA^{1/3},a_o)$ where V_c is the Coulomb potential. The values of the parameters are from Ref.[7]. The $(W-S)^2$ type is of the form :
$V(r) = V_c - V_o[f(r,r_o\ A^{1/3}, a_o)]^2 - iWf(r,r_oA^{1/3},a_o)$ where the values of the parameters are taken from Ref.[9].

Table 3 : Results of the CRC analysis

Low-lying strong collective states in ^{42}Ca[a)]			Levels of ^{43}Ca observed in the present work and considered in CRC calculations			
J^{π}	E_x (MeV)	δ (fm)	multiplet	J^{π}	E_x (MeV)	σ_{exp}/σ_{th} [b)]
2^+	1.52	1.06	$2^+ \otimes f_{7/2}$	$\frac{11}{2}^-$	1.678	(0.04)
				$\frac{9}{2}^-$	2.247	0.70
				$\frac{11}{2}^-$	3.044	0.06
4^+	2.75	0.37	$4^+ \otimes f_{7/2}$	$\frac{13}{2}^-$	3.645	3
3^-	3.44	0.95	$3^- \otimes f_{7/2}$	$\frac{3}{2}^+$	0.990	8.5
				$\frac{1}{2}^+$	1.957	3
				$\frac{1}{2}^+$	2.741	1
				$\frac{3}{2}^+$	2.850	2.1
				$\frac{11}{2}^+$	2.952	0.5
				$\frac{13}{2}^+$	3.371	0.11
				$\frac{13}{2}^+$	3.504	0.13
				$(\frac{7}{2})^+$	5.251	3.2

a) Ref.[14)]. The deformation length λ is the product of the deformation parameter β and the radius $r_o A^{1/3}$ in the real part of the optical potential.

b) The ratio σ_{exp}/σ_{th} should be equal to 1 in a pure weak-coupling scheme.

Figure captions

Fig. 1 : ^{3}He energy spectrum from $^{42}Ca(\alpha,{}^{3}He)^{43}Ca$ reaction at 14° laboratory, given by a 50 cm delay line gaz counter. The numbers on the top of the peaks refer to the ^{43}Ca levels reported in Table 1. The hatched peaks are from contaminants.

Fig. 2 : DWBA predictions using two different α-optical potentials reported in Table 2, for two sets of states in ^{43}Ca (this work) and in ^{41}Ca (Paper I[1]) .

Fig. 3 : Comparison of experimental angular distributions with DWBA predictions for ℓ = 1,2 and 3 direct transfers to states below 4 MeV excitation energy in ^{43}Ca. The α-potential used here is that of W-S type.

Fig. 4 : Comparison of experimental angular distributions with DWBA predictions for ℓ = 3 and 4 direct transfers to states at high excitation energy. Two α-potentials reported in Table 2 were used.

Fig. 5 : Comparison of experimental angular distributions of the weakly excited states in ^{43}Ca with purely two-step CRC (full line) predictions normalized to the data. The dotted lines are specified in the figure.

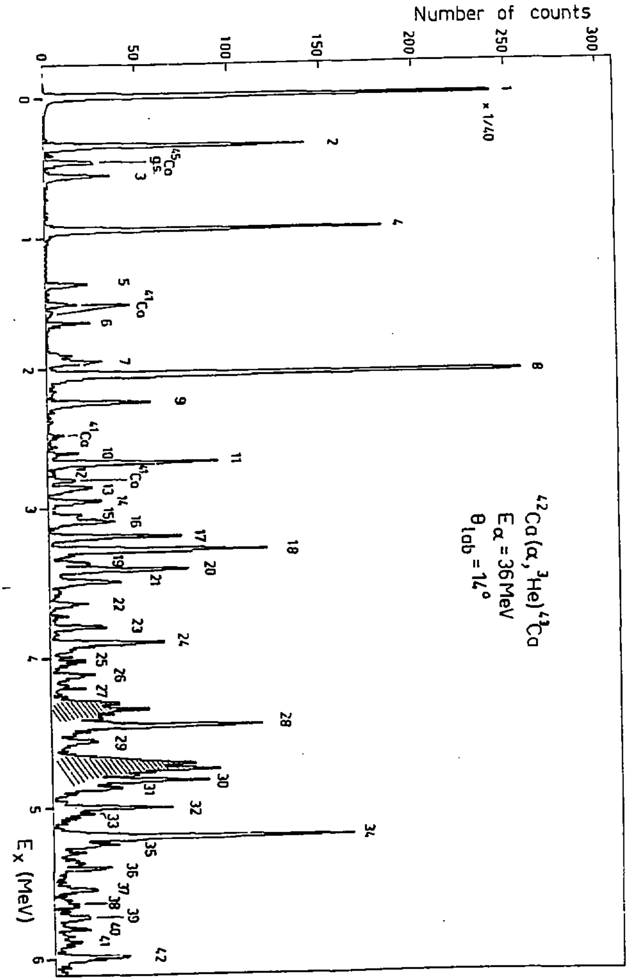

Fig. 1

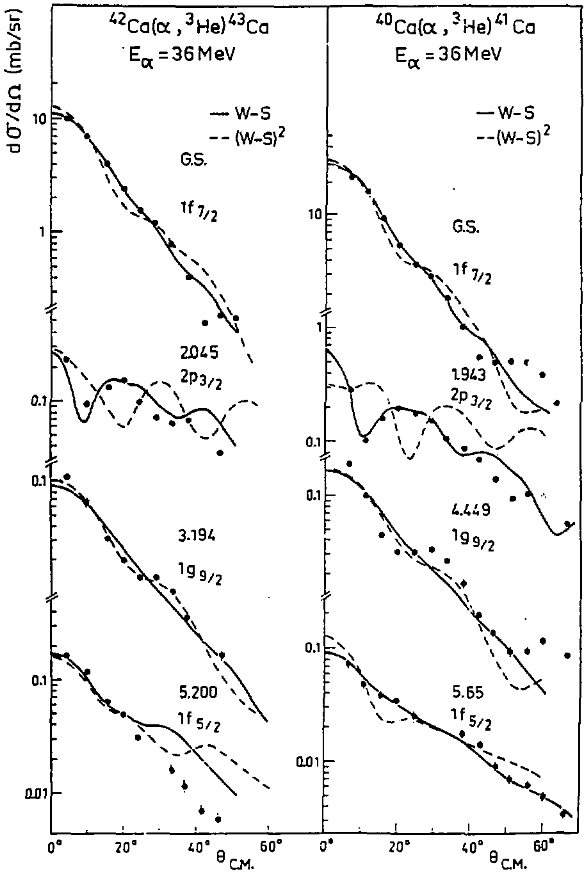
$^{42}Ca(\alpha, {}^3He)^{43}Ca$
$E_\alpha = 36$ MeV
$^{40}Ca(\alpha, {}^3He)^{41}Ca$
$E_\alpha = 36$ MeV
dσ/dΩ (mb/sr)
— W-S
-- $(W-S)^2$
G.S.
$1f_{7/2}$
2.045
$2p_{3/2}$
3.194
$1g_{9/2}$
5.200
$1f_{5/2}$
1.943
$2p_{3/2}$
4.449
$1g_{9/2}$
5.65
$1f_{5/2}$
10
1
0.1
0.01
0° 20° 40° 60°
$\theta_{C.M.}$

Fig. 2

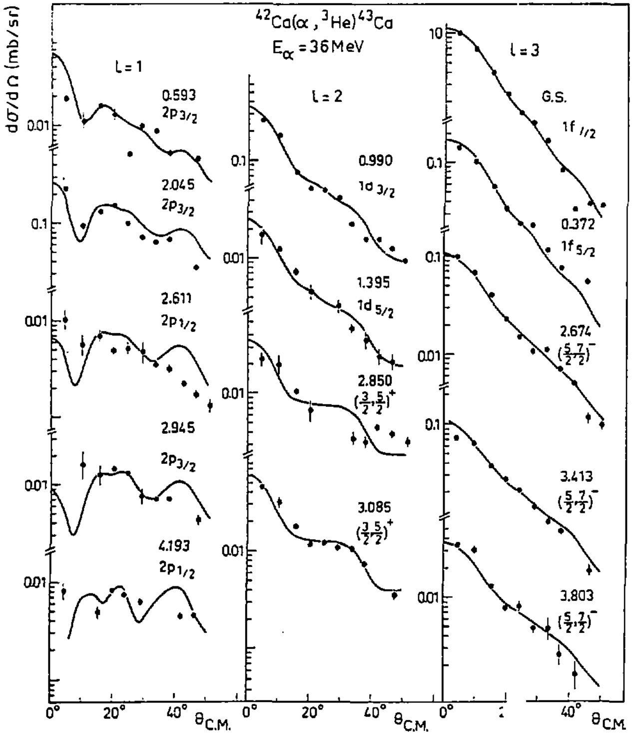

$^{42}Ca(\alpha, {}^3He)^{43}Ca$
$E_\alpha = 36$ MeV
dσ/dΩ (mb/sr)
l = 1
l = 2
l = 3
0.593
$2p_{3/2}$
2.045
$2p_{3/2}$
2.611
$2p_{1/2}$
2.945
$2p_{3/2}$
4.193
$2p_{1/2}$
0.990
$1d_{3/2}$
1.395
$1d_{5/2}$
2.850
$(\frac{3}{2},\frac{5}{2})^+$
3.085
$(\frac{3}{2},\frac{5}{2})^+$
G.S.
$1f_{7/2}$
0.372
$1f_{5/2}$
2.674
$(\frac{5}{2},\frac{7}{2})^-$
3.413
$(\frac{5}{2},\frac{7}{2})^-$
3.803
$(\frac{5}{2},\frac{7}{2})^-$
$\theta_{C.M.}$

Fig. 3

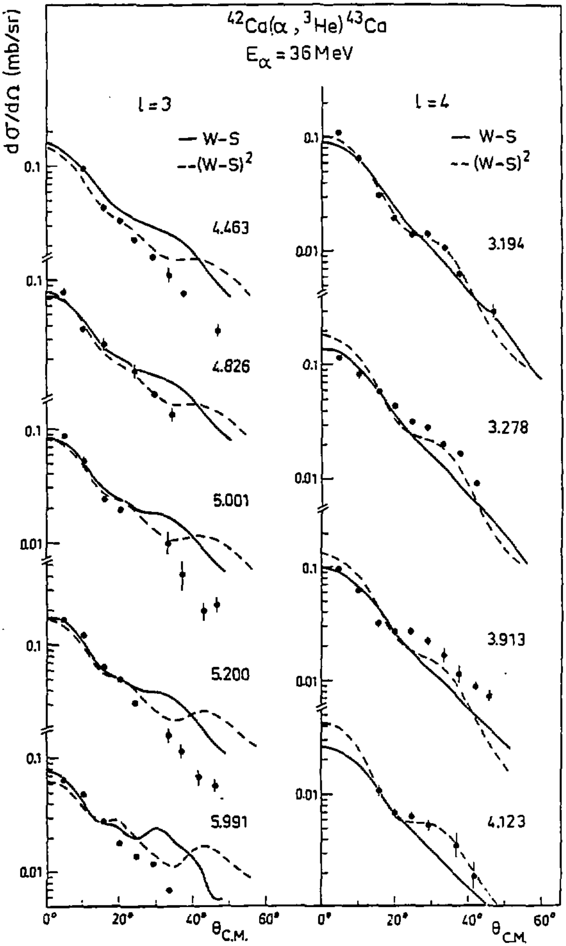

42Ca(α, 3He)43Ca
Eα = 36 MeV
dσ/dΩ (mb/sr)
l = 3
— W-S
-- (W-S)2
l = 4
4.463
4.826
5.001
5.200
5.991
3.194
3.278
3.913
4.123
0.1
0.01
0°
20°
40°
60°
θC.M.

Fig. 4

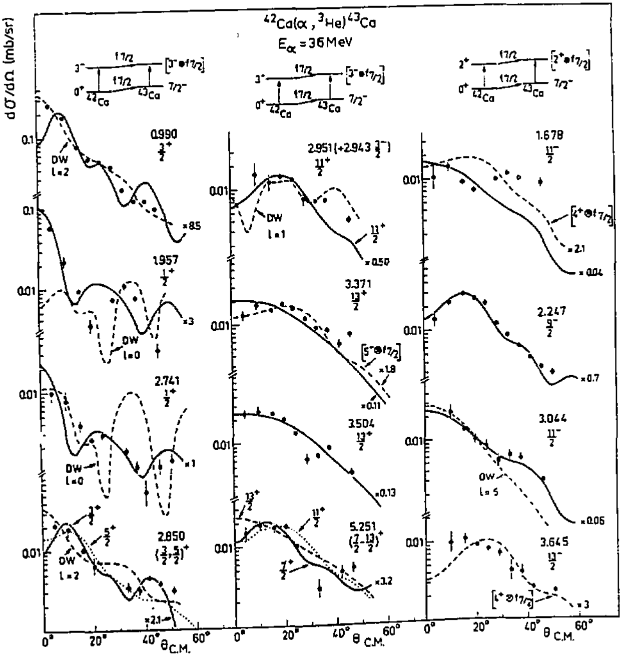

$^{42}Ca(\alpha, {}^3He)^{43}Ca$
$E_\alpha = 36$ MeV
$d\sigma/d\Omega$ (mb/sr)
$\theta_{C.M.}$

Fig. 5